Coexisting Attractors and Their Control in an Angular Motion Transfer Mechanism

MINVYDAS RAGULSKIS
Department of Mathematical Research in Systems, Kaunas University of Technology, Kaunas, LT-3028, Lithuania

(Received 23 July 2002; accepted 9 October 2002)

Abstract: It is shown that even simple models of angular motion transfer mechanisms possess features characteristic to non-linear dynamical systems: coexistence of periodic attractors, non-synchronous motion modes, chaotic solutions. Some of those features are quite unique. The transition to chaos takes place when the damping of the output element is increased. The basin boundaries of strange attractors are not fractal. The existence of multiple stable attractors enables the design of a new type of control strategy for angular motion transfer mechanisms.

Key Words: Chaos, coexisting attractors, control

1. INTRODUCTION

The analysis of inertia-type rotary motion transfer mechanisms has a long history and traditions. Various modifications of these mechanisms are studied and developed. However, most attention has been given to the stability of the systems, the ability of clutches to damp hazard vibrations around the steady rotation and the ability of output elements to follow the changes of the revolution frequency of the input shaft (Poliakov and Barbash, 1973; Centea et al., 2001).

Nevertheless, little attention has been dedicated to the analysis of "degenerated" modes of motion when the output element of the coupling does not follow the motion of the input element. Such motions have low practical value for many types of coupling and may even lead to the damage of constructions.

The object of this paper is to show that certain types of inertia couplings may possess stable non-synchronous motions. Understanding the dynamic properties of such mechanisms is an interesting task from the theoretical point of view. Also, it may lead to practical applications exploiting the non-linear effects taking place in the analyzed systems.

2. MODEL OF THE SYSTEM AND DIFFERENTIAL EQUATIONS OF MOTION

A planar rotary motion transfer mechanism consisting of input and output elements is analyzed (Figure 1). The input element can rotate around the axis O_1; the output element

Journal of Vibration and Control, **10:** 101–113, 2004 DOI: 10.1177/107754604031475

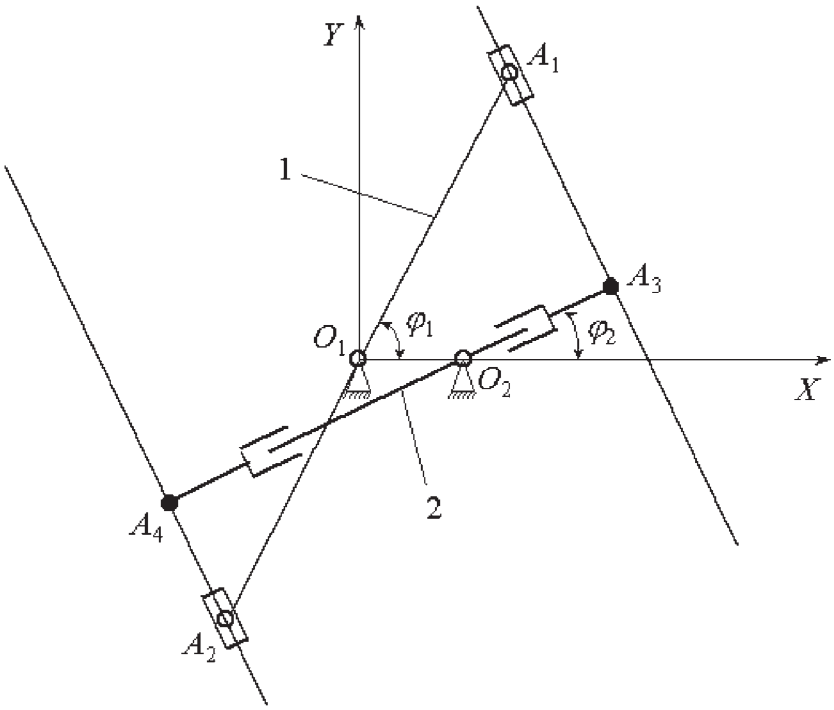

Figure 1. Schematic diagram of the rotary motion transfer mechanism: 1, input element; 2, output element.

around the axis O_1. The eccentricity (distance between the axes of rotation of the input and output elements) is denoted as E; $|O_1A_1| = |O_1A_1| = R$. It is assumed that the points O_1 and O_1 lie on the frame axis $0X$ (Figure 1). Points $A_1O_1A_1$ and $A_3O_1A_4$ always lie on straight lines. The ends of the input element can rotate and slide on the guides of the output element. These guides are perpendicularly jointed to the axis of rotation of the output element by viscous dampers: $(A_1A_3)\perp(A_3O_1A_4)$ and $(A_1A_4)\perp(A_3O_1A_4)$. The mass of the system is concentrated in two points: A_3 and A_4. It is clear that the rotation of the input element will bring the output element into rotation and the presented mechanism can be interpreted as a rotary motion transfer coupling.

The distances $|O_1A_3|$ and $|O_1A_4|$ can be expressed as

$$\begin{aligned} |O_1A_3| &= R\cos(\varphi_1 - \varphi_1) - E\cos\varphi_1 \\ |O_1A_4| &= R\cos(\varphi_1 - \varphi_1) + E\cos\varphi_1, \end{aligned} \tag{1}$$

where φ_1 and φ_1 denote the angles of rotation of the input and the output elements, respectively.

The coordinates of points $A_3\left\{X_3, Y_3\right\}$ and $A_4\left\{X_4, Y_4\right\}$ are

$$\begin{aligned} X_3 &= \left|O_1A_3\right|\cos\varphi_1 + E \\ Y_3 &= \left|O_1A_3\right|\sin\varphi_1 \\ X_4 &= -\left|O_1A_4\right|\cos\varphi_1 + E \\ Y_4 &= -\left|O_1A_4\right|\sin\varphi_1. \end{aligned} \tag{2}$$

Elementary transformations lead to the following expression of the kinetic energy of the system

$$T = 0.5J_1\dot{\varphi}_1^1 + 0.5J_1\dot{\varphi}_1^1 + m\dot{\varphi}_1^1\left(E^1 + R^1\right) + mR^1\left(\dot{\varphi}_1^1 - 2\dot{\varphi}_1\dot{\varphi}_1\right)\sin^1\left(\varphi_1 - \varphi_1\right), \tag{3}$$

where J_1 and J_1 are moments of inertia of the input and output elements, *m* is the concentrated mass, and top dots denote derivatives by time *t*.

Then, the inertia terms of the differential equations can be expressed as

$$\begin{aligned} J\left(\varphi_1\right) &= \frac{d\left(\dfrac{\partial T}{\partial\dot{\varphi}_1}\right)}{dt} - \frac{\partial T}{\partial\varphi_1} \\ &= J_1\ddot{\varphi}_1 + 2mR^1\left(\left(\ddot{\varphi}_1 - \ddot{\varphi}_1\right)\sin\left(\varphi_1 - \varphi_1\right)\right. \\ &+ \left.\left(\dot{\varphi}_1^1 - 2\dot{\varphi}_1\dot{\varphi}_1 + 2\dot{\varphi}_1^1\right)\cos\left(\varphi_1 - \varphi_1\right)\right)\sin\left(\varphi_1 - \varphi_1\right) \end{aligned} \tag{4}$$

$$\begin{aligned} J\left(\varphi_1\right) &= \frac{d\left(\dfrac{\partial T}{\partial\dot{\varphi}_1}\right)}{dt} - \frac{\partial T}{\partial\varphi_1} \\ &= \left(J_1 + 2m\left(E^1 + R^1\right)\right)\ddot{\varphi}_1 - 2mR^1\left(\ddot{\varphi}_1\sin\left(\varphi_1 - \varphi_1\right)\right. \\ &+ \left.\dot{\varphi}_1^1\cos\left(\varphi_1 - \varphi_1\right)\right)\sin\left(\varphi_1 - \varphi_1\right). \end{aligned} \tag{5}$$

The energy of forces of dissipation is

$$D = 0.5H\left(\left(\frac{d\left|O_1A_3\right|}{dt}\right)^1 + \left(\frac{d\left|O_1A_4\right|}{dt}\right)^1\right) + 0.5\left(H_1\dot{\varphi}_1^1 + H_1\dot{\varphi}_1^1\right), \tag{6}$$

where H_1 and H_1 are the coefficients of viscous damping of the input and output elements, respectively.

Partial derivatives take the form:

$$\begin{aligned}\frac{\partial D}{\partial \dot{\varphi}_1} &= 2HR^1\left(\dot{\varphi}_1-\dot{\varphi}_1\right)\sin^1\left(\varphi_1-\varphi_1\right)+H_1\dot{\varphi}_1\\ \frac{\partial D}{\partial \dot{\varphi}_1} &= -2HR^1\left(\dot{\varphi}_1-\dot{\varphi}_1\right)\sin^1\left(\varphi_1-\varphi_1\right)+2HE^1\dot{\varphi}_1\sin^1\varphi_1+H_1\dot{\varphi}_1.\end{aligned} \tag{7}$$

The resulting differential equations of motion are

$$\begin{cases} J\left(\varphi_1\right)+\dfrac{\partial D}{\partial \dot{\varphi}_1}=M_1\\ J\left(\varphi_1\right)+\dfrac{\partial D}{\partial \dot{\varphi}_1}=M_1, \end{cases} \tag{8}$$

where M_1 and M_1 denote the external moments acting to the input and output elements.

When the input element moves with constant velocity $\varphi_1 = \omega t$, and there is no external moment applied to the output element, the resulting one-degree-of-freedom system is described by the following equation:

$$\begin{aligned} & \left(J_1+2m\left(E^1+R^1\right)\right)\ddot{\varphi}+H_1\dot{\varphi}\\ = \; & mR^1\omega^1\sin 2\left(\omega t-\varphi\right)+HR^1\left(\omega-\dot{\varphi}\right)\left(1-\cos 2\left(\omega t-\varphi\right)\right)\\ - \; & HE^1\dot{\varphi}\left(1-\cos 2\varphi\right). \end{aligned} \tag{9}$$

The introduction of variables $x = 2\varphi$ and $\tau = 2\omega t$ transforms equation (9) to the following form

$$\ddot{x}+h\dot{x}=a\sin\left(\tau-x\right)+Hb\left(1-\dot{x}\right)\left(1-\cos\left(\tau-x\right)\right)-HE^1c\dot{x}\left(1-\cos x\right), \tag{10}$$

where

$$\begin{aligned} h &= \frac{H_1}{2\omega\left(J_1+2m\left(E^1+R^1\right)\right)};\\ a &= \frac{mR^1}{2\left(J_1+2m\left(E^1+R^1\right)\right)};\\ b &= \frac{R^1}{2\omega\left(J_1+2m\left(E^1+R^1\right)\right)}; \end{aligned}$$

$$c = \frac{1}{2\omega\left(J_1 + 2m\left(E^1 + R^1\right)\right)}.$$

By the way, it can be noted that $0 \leq a \leq 0.25$.

When $H = 0$, equation (10) takes the form:

$$\ddot{x} + h\dot{x} = a \sin\left(\tau - x\right). \tag{11}$$

3. MULTIPLE SOLUTIONS AND THEIR BASIN BOUNDARIES WHEN $H = 0$

The trivial solution of equation (11) is

$$x = \tau + \alpha, \tag{12}$$

where α is constant (it is assumed that $h \geq 0$ and $a \geq 0$). The necessary condition of existence of this solution is

$$h < a. \tag{13}$$

The stability of this solution can be defined from the equation in variations in the infinitesimal of α ($\alpha = \alpha + \delta\alpha$):

$$\delta\ddot{\alpha} + h\delta\dot{\alpha} + a\cos\alpha\delta\alpha = 0. \tag{14}$$

The trivial solution is unstable (a saddle point) when $\alpha = -\arcsin\left(h/a\right) + 2\pi k$, and stable when $\alpha = \arcsin\left(h/a\right) + \pi\left(2k+1\right)$. The sign of the radical of the characteristic equation (14) defines the type of the stable solution; it is the focus type attractor when

$$h^1/4 < \cos\alpha, \tag{15}$$

and the knot type attractor when

$$h^1/4 \geq \cos\alpha. \tag{16}$$

The boundary line separating these two types of stable attractor in the parameter plane $a - h$ can be found from equations (16) and (11):

$$a^1 = h^4/16 + h^1. \tag{17}$$

The trivial solution is a default operation mode for eccentric clutch coupling mechanisms. The output element follows the steady motion of the input element with certain backwardness, which is constant in time.

As the trivial solution (12) does not exist when the inequality (13) is not satisfied, it is clear that this is not the only solution of the system. Numerical investigations prove the

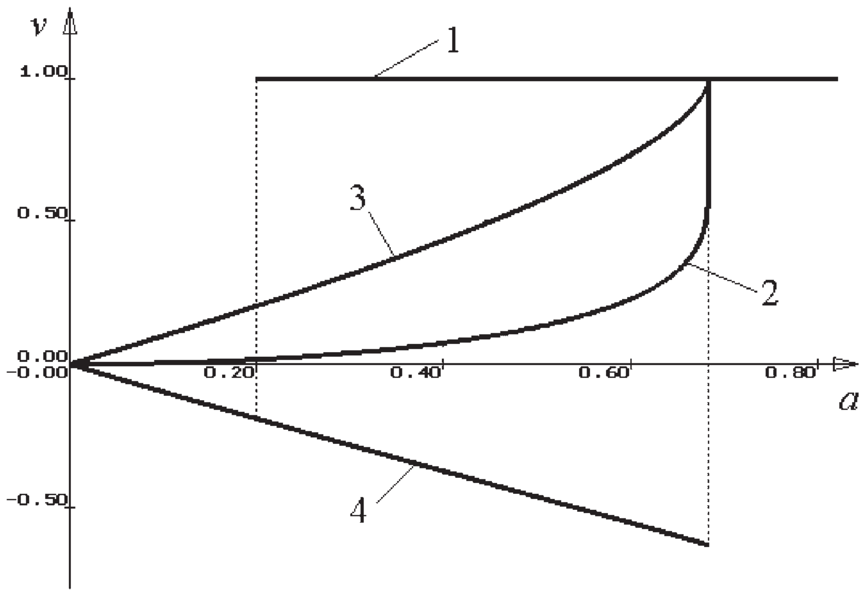

Figure 2. Coexistence of attractors at $h = 0.2$. Line 1 represents the velocity of the trivial solution; lines 2, 3 and 4 represent average, maximum and minimum velocities per period of small average velocity solution.

existence of another solution. It is a stable periodic attractor (in phase plane $\dot{x} - \ddot{x}$) with positive average velocity (Figure 2). Moreover, this solution can coexist with the trivial solution in a certain region of the parameter plane. In such a case, the multiple attractors are sensitive to the initial conditions (Figure 3). The picture of basin boundaries of attractors is periodic by 2π and can be represented in cylindrical coordinates, but the clarity of the view is then lost.

The non-existence of the small negative average velocity solution can be interpreted by the following considerations. The change of variables

$$z = \tau - x \tag{18}$$

transforms equation (11) to the following form:

$$\ddot{z} + h\dot{z} + a \sin z = h. \tag{19}$$

At $h = 0$, equation (19) describes the motion of a non-linear pendulum (Zaslavsky at al., 1991).

When $h \neq 0$, the map of basin boundaries of coexisting attractors is presented in Figure 3. The map is not symmetric with respect to the z-axis, moreover, the boundary lines do not form closed structure; the region of initial conditions tending to the trivial solution is opened to infinity in the upper part of the phase plane. Thus, the only possible stable infinite trajectory

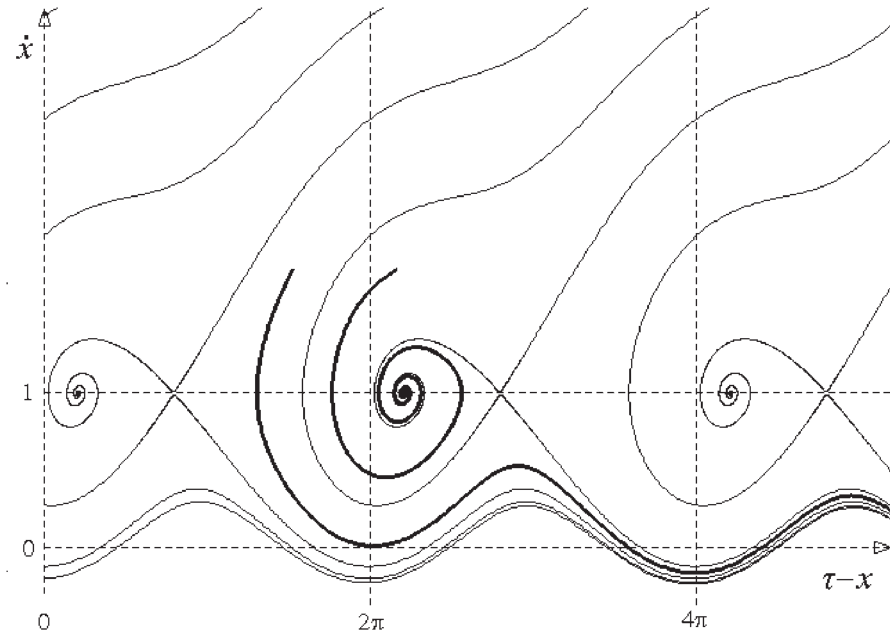

Figure 3. Basin boundaries of coexisting attractors at $h = 0.2$, $a = 0.25$. The two thick solid lines represent the transient processes from different initial conditions.

is located under the boundary. There does not exist symmetric infinite trajectory with negative average velocity.

The non-trivial solution can be approximated using analytical techniques. If the average velocity of the steady-state attractor is denoted as v, and $v \to 0$, the solution can be approximated by a sum of harmonic oscillations and constant velocity motion:

$$x \approx v\tau + b \sin\left((1-v)\,\tau\right). \tag{20}$$

The following approximations can be produced from equations (18) and (11):

$$\begin{aligned} v &\approx 0.5a^1/\left(1+h^1\right), \\ b &\approx a\left(\left(1-v^1\right)+h^1\right)^{-1}. \end{aligned} \tag{21}$$

When $v \to 1$, the non-trivial solution can be interpreted as a soliton-type solution similar to the motion of the non-linear pendulum in the vicinity of the boundary between rotational and vibrational modes of motion (Zaslavsky et al., 1991). The solution remains for relatively long time periods in the surroundings of an unstable saddle point, and then quickly jumps to the next saddle point in the phase plane $\dot{x}$, $(\tau - x)$. When $0 < v < 1$, the small average velocity attractor can be interpreted as a combination between those too extreme variants.

It can be noted that the system described by equation (11) does not possess chaotic solutions, as it does not satisfy the minimum requirements for having these (Ott, 1993); the system is described by less than three independent variables and all functions are smooth and differentiable. An important conclusion can be made from the presented reasoning: the existence of eccentricity will not develop chaotic motions of the described mechanism when $H = 0$.

4. MULTIPLE SOLUTIONS AND TRANSITION TO CHAOS AT $H \neq 0$

When $H \neq 0$ and $E = 0$, equation (11) does not produce chaotic solutions either; the status of the system is defined by two independent quantities, $(\tau - x)$ and $\dot{x}$. The multiple attractors also can coexist, although the damping forces in the output link alter the low average velocity attractor; the average velocity is increased compared to the non-damped solution, and the minimum and maximum velocities in the period are also increased. The minimum velocity in the steady-state period is not necessarily negative.

The structure of the solution is more complex when both parameters H and E are not equal to zero. The status of the system is defined by three independent quantities: $(\tau - x)$, x and $\dot{x}$.

There are many different known ways for the transition of solutions to chaos. Those transitions are usually observed when one or several parameters of the analyzed system are gradually changed, and the steady-state solution runs through cascades of bifurcations (Ding et al., 1989; Yu et al., 1991). However, as is common for non-linear mechanical systems, chaotic solutions may occur if the damping is small enough (Fendel et al., 1998; Ott, 1993; Zaslavsky et al., 1991).

The analyzed mechanism (Figure 1) is a kind of exception from the rule. Transition to stochasticity and chaotic motions take place when the damping coefficients in the output element are increased. This can be understood from the structure of differential equations, but is far from being trivial if the design of the mechanism is considered. Numerical modeling proves the fact; Figure 4 represents the Poincaré map of steady-state motion. For every single value of H, equation (9) is integrated using the time marching method until the transient processes cease. Then, 10 000 time steps are used to construct the Poincaré points (attractor in the phase plane $\dot{\varphi} - \ddot{\varphi}$ is sliced by the line $\ddot{\varphi} = 0$). Moreover, two solutions for different initial conditions are calculated and represented for every single value of H. At $H = 0$, two attractors coexist (Figure 4); the trivial solution is represented by a point at 1.0, and the small average velocity periodic solution is represented by two points on the vertical axis. Increment of H distorts the attractors; the trivial solution turns out to be a deterministic periodic attractor with the average velocity equal to one. Further increase of H terminates the existence of this atttractor, and only the small average velocity attractor exists.

The shapes of coexisting attractors are represented in Figures 5 and 6. The positions of the input and output elements are frozen at certain time moments, while the thin solid lines represent the trace of the points A_3 and A_4 in time. By the way, it can be noted that the Poincaré maps are constructed not from that trace, but from the attractors in the phase plane $\dot{\varphi} - \ddot{\varphi}$.

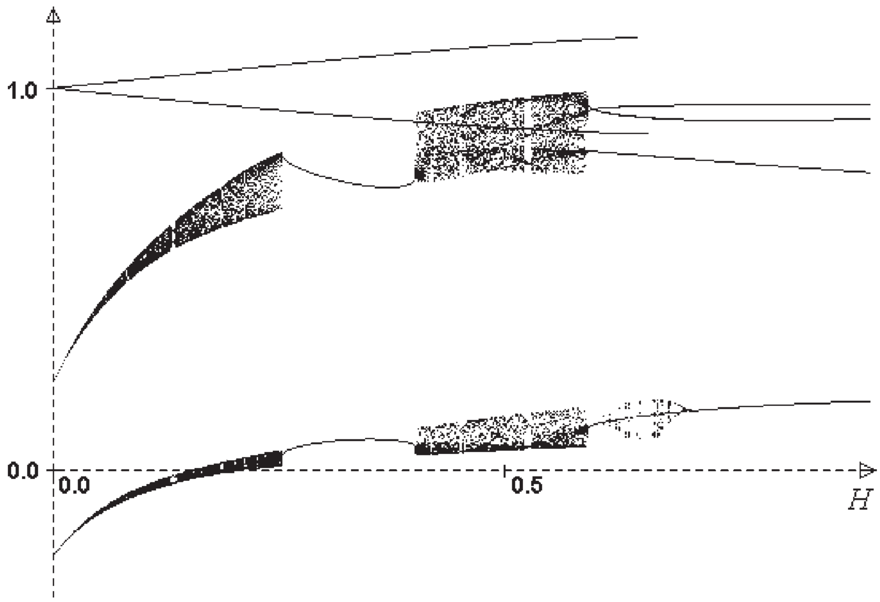

Figure 4. Poincaré map of the steady-state attractors at $h = 0.1$, $a = 0.2$, $E = 0.7$, $b = 0.4$, $c = 0.4$.

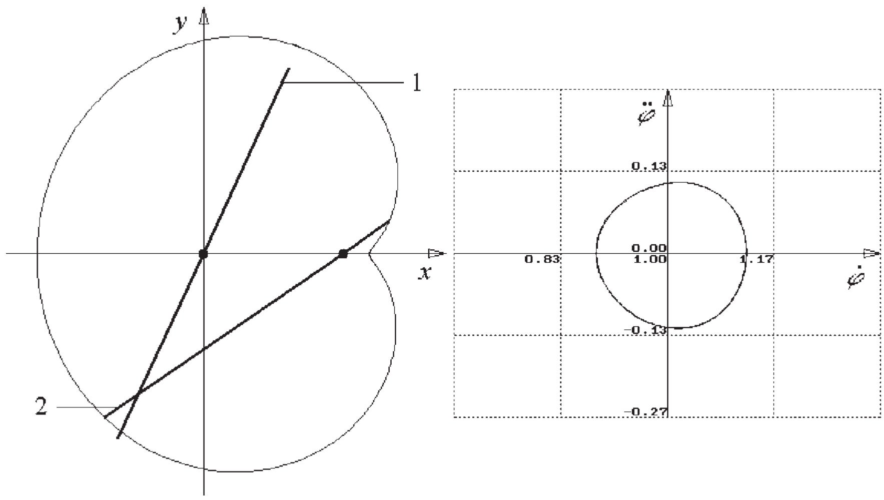

Figure 5. Periodic attractor with average velocity equal to one: the trace of concentrated masses (1, the input element; 2, the output element) and the orbit in phase plane $\dot{\varphi} - \ddot{\varphi}$ at $H = 0.5$, $h = 0.1$, $a = 0.2$, $E = 0.7$, $b = 0.4$, $c = 0.4$.

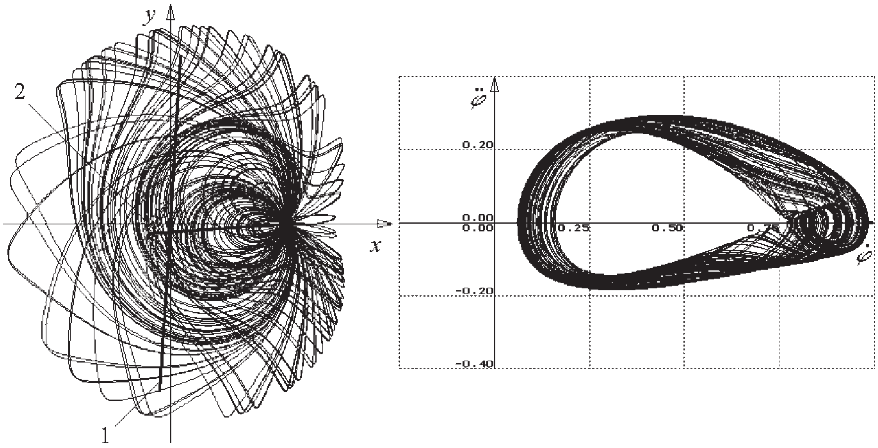

Figure 6. Small average velocity attractor: the trace of concentrated masses (1, the input element; 2, the output element) and the orbit in phase plane $\dot{\varphi} - \ddot{\varphi}$ at $H = 0.5$, $h = 0.1$, $a = 0.2$, $E = 0.7$, $b = 0.4$, $c = 0.4$.

The period of the high average velocity attractor coincides with the cycle of revolution of the driving input element, while the period of the small average velocity attractor is longer and depends on the average velocity of the output element.

Another interesting property of the analyzed system is the fact that the basin boundaries of the coexisting attractors are not fractal. As the analytical determination of unstable solution of equation (10) is very complicated, the basin boundaries are constructed performing full sorting of initial conditions. It can be noted that the shape of boundaries in principle is analogous to the structure of boundaries for the differential equation (11).

5. CONTROL OF MULTIPLE REGIMES OF MOTION

The existence of a stable motion mode with relatively small average velocity forms a potential possibility for existence of “degenerated” modes of motion, as the average angular velocity of the output element is smaller than the angular velocity of the input element. By the way, variation of the parameter H can control the average velocity of the output element.

As the coexisting regimes of motion are sensitive to the initial conditions, it is clear that external effects such as shocks can bring the motion of the output system from one regime of motion to another. For example, a single external shock can bring the state of the output element from the boundaries of attraction to the trivial solution. Then, a special motion control strategy is necessary for bringing the output element back to the desired regime of motion.

The motion of the output element can be controlled by an external force impulse applied in the direction of rotation of the input element. This can be illustrated by Figures 7 and 8, where the motion of the output element is brought back from the small average velocity attractor to the basin of attraction of the trivial solution. It can be noted that the magnitude

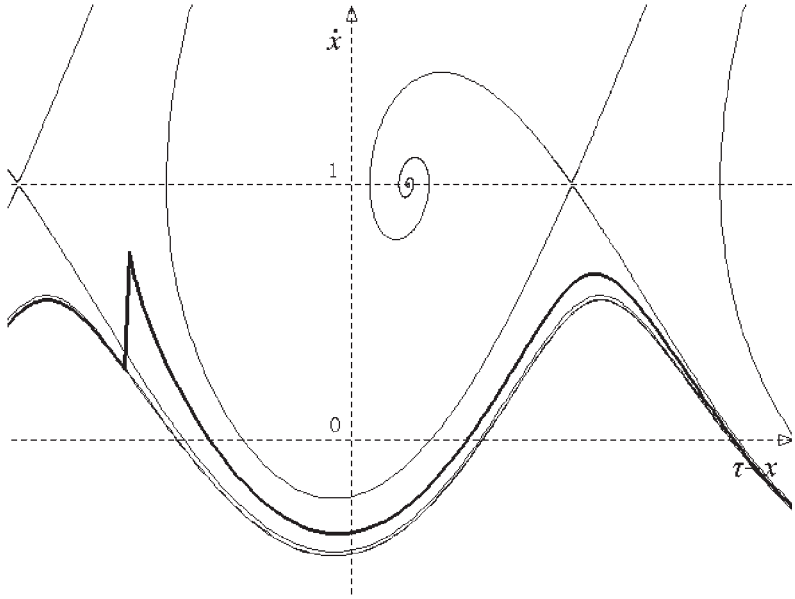

Figure 7. Effect of external impulse to the transient dynamics at $h = 0.2$, $a = 0.25$.

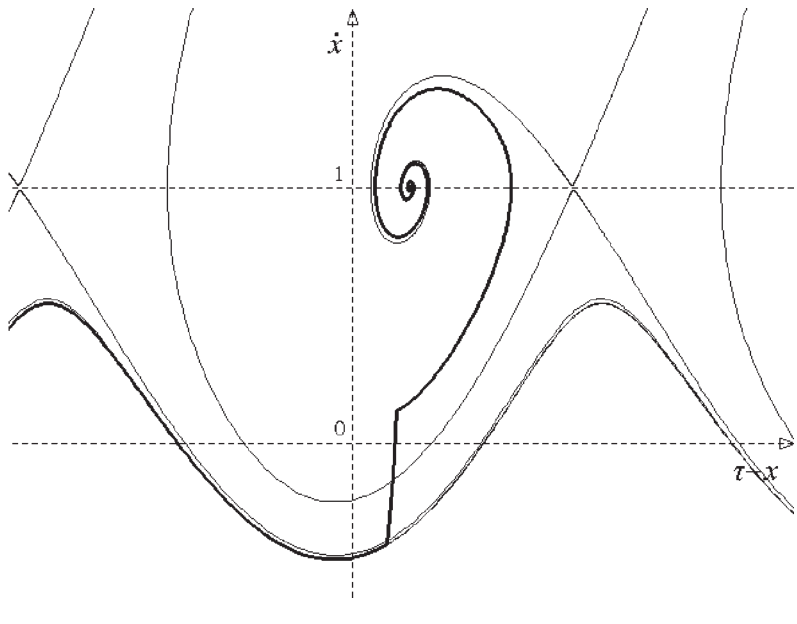

Figure 8. Effect of external impulse to the transient dynamics at $h = 0.2$, $a = 0.25$ (different phase when the impulse is applied).

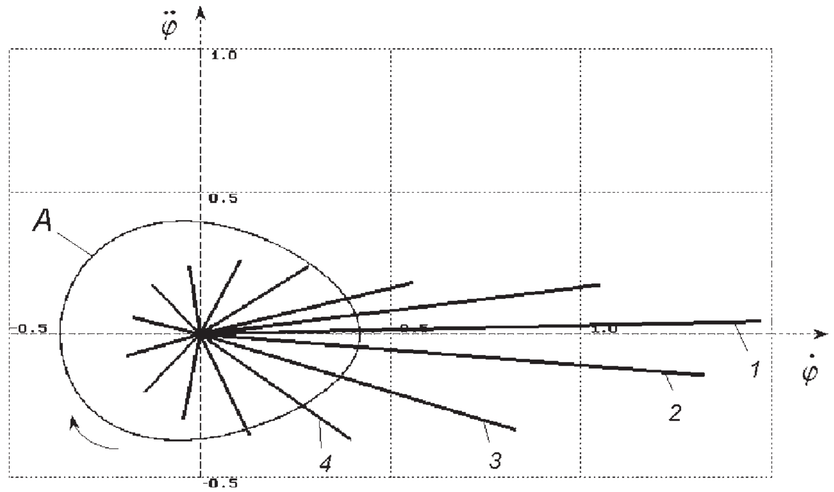

Figure 9. Minimal required impulses for bringing the system to the trivial regime of motion at $h = 0.2$, $a = 0.25$.

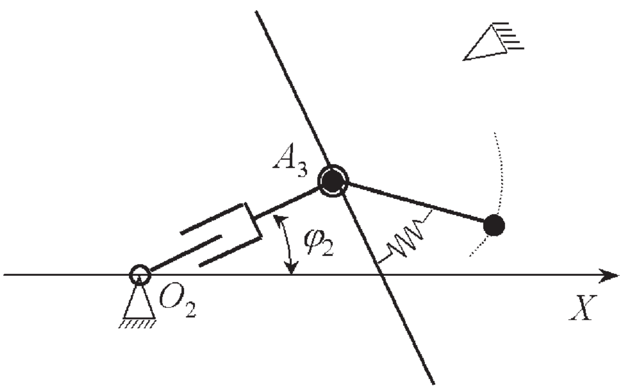

Figure 10. Schematic diagram of a contrivance device for the elimination of trivial solution in the region of coexisting attractors.

of the minimal impulse necessary for such transition depends on the relative phase of the output element at the moment when the external impulse is applied. Quite unexpected is the fact that the minimum required magnitude of the impulse is not smallest when the velocity of the output element is highest in its orbit in the phase plane $\dot{\varphi} - \ddot{\varphi}$. This fact is illustrated in Figure 9 (the phase interval is split into 15 uniform intervals) and can be important for practical applications if the motion control of the output element of the clutch is considered in the region of coexistence of multiple attractors.

Alternatively, the presented system can serve as a non-synchronous angular motion transfer mechanism. The average angular velocity of the output element can be varied at constant angular velocity of the input element; if the control parameter h is appropriately varied (Figure 2). In this sense the presented mechanism can serve as a drive without stages. By the way, the unevenness of the small average velocity regime of motion can be decreased by additional dynamical elements.

It can be noted that the control of regimes of motion in that case can be implemented using simple mechanical contrivance as shown in Figure 10. When the output element approaches the angular speed of the input element, the inertia mass attached to the output element by a spring will be bent up and will hit the motionless support. That impulse would bring the output element back to the small average velocity regime of motion. The eccentric mass and the spring of this control element can be selected to enable the rotation of the output element without hitting the support when it performs the angular motion slower than that of the input element.

6. CONCLUSIONS

The presented rotary motion transfer mechanism is shown to possess a range of specific non-linear features: coexistence of periodic attractors, chaotic motion modes. Some of these features are quite unique and make the analyzed system different from the whole class of non-linear mechanical systems. The transition to chaos takes place when the damping in the output element is increased. The eccentricity by itself is not sufficient for originating stochastic motions. If the stochastic attractors exist, their basin boundaries are not fractal. Finally, the method of control of multiple regimes of motion is proposed.

REFERENCES

Centea, D., Rahnejat, H., and Menday, M. T., 2001, “Non-linear multi-body dynamic analysis for the study of clutch torsional vibrations,” *Applied Mathematical Modelling* **25**(3), 177.

Ding, M., Grebogi, C., and Ott, E., 1989, “Evolution of attractors in quasi-periodically forced systems: from quasi-periodic to strange non-chaotic to chaotic,” *Physical Review A* **39**, 2593.

Feudel, U., Grebogi, C., Poon, L., and Yorke, J. A., 1998, “Dynamic properties of a simple mechanical system with a large number of coexisting periodic attractors,” *Chaos, Solitons and Fractals* **9**, 171.

Ott, E., 1993, *Chaos in Dynamical Systems*, Cambridge University Press, London.

Poliakov, V. S. and Barbash, I. D., 1973, *Clutches. Design and Analysis*, Mashinostroenie, Leningrad.

Yu, L., Ott, E., and Chen, Q., 1991, “The transition to chaos for random dynamical systems,” *Physical Review Letters* **65**, 2935.

Zaslavsky, G. M., Sagdeev, R. Z., Usikov, D. A., and Chernikov, A. A., 1991, *Weak Chaos and Quasi-Regular Patterns,* Nauka, Moscow.